**Cell Reports, Volume *23***

## Supplemental Information

# Psychedelics Promote Structural and Functional Neural Plasticity

**Calvin Ly, Alexandra C. Greb, Lindsay P. Cameron, Jonathan M. Wong, Eden V. Barragan, Paige C. Wilson, Kyle F. Burbach, Sina Soltanzadeh Zarandi, Alexander Sood, Michael R. Paddy, Whitney C. Duim, Megan Y. Dennis, A. Kimberley McAllister, Kassandra M. Ori-McKenney, John A. Gray, and David E. Olson**

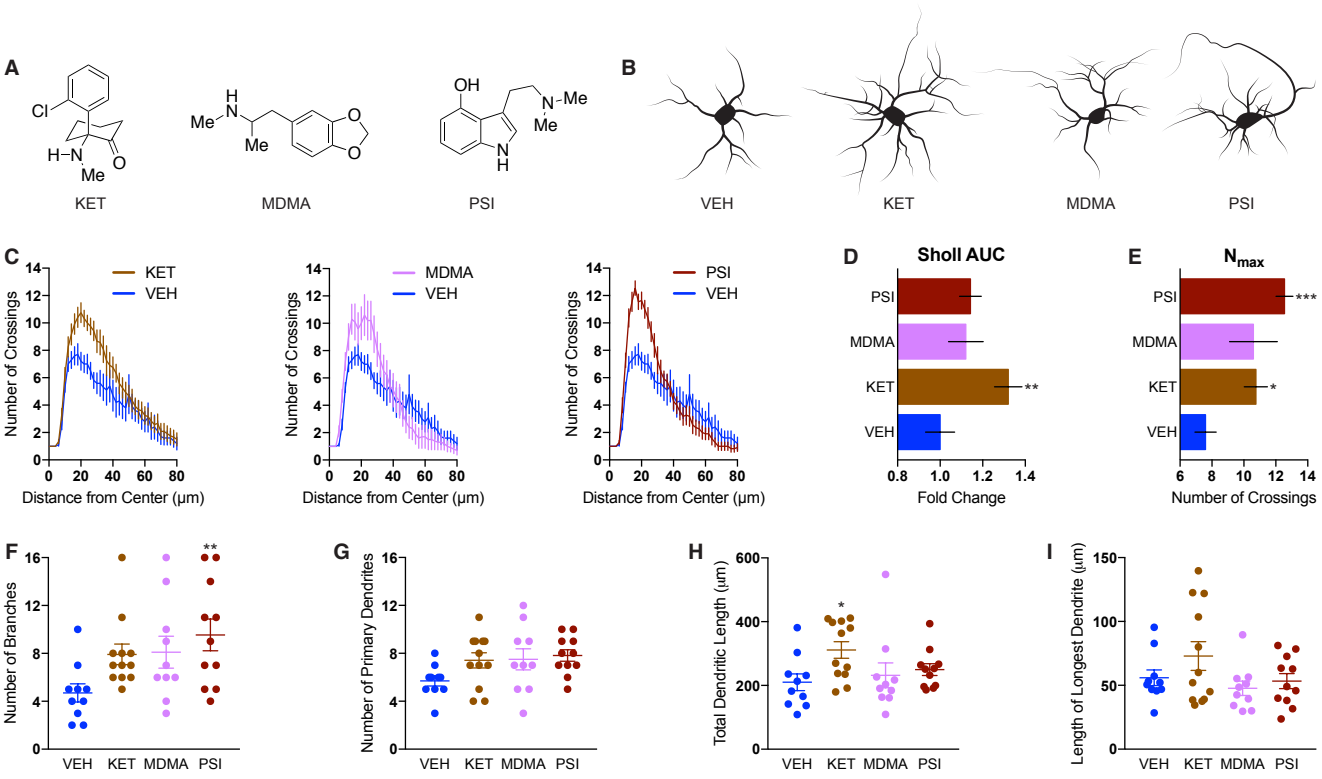


**Figure S1. Psychedelics Promote Neuritogenesis (Additional Compounds), Related to Figure 1.** (A) Chemical structures of additional psychedelics used in these studies. (B) Representative tracings of cultured embryonic rat cortical neurons (DIV6) treated with compounds. (C) Sholl analysis (circle radii = 2 μm increments) demonstrates that cultured cortical neurons treated with several psychedelics have more complex dendritic arbors as compared to vehicle control (n = 10–12 neurons per treatment). (D) Area under the curve (AUC) of the Sholl plots in C. (E) Maximum number of crossings ($N_{max}$) of the Sholl plots in C. (F–I) Cultured cortical neurons treated with several psychedelics display a trend towards an increase in the number of branch points (F), the number of primary dendrites (G), and the total length of the dendritic arbor (H), but not the length of the longest dendrite (I). Error bars represent s.e.m. *P < 0.05, **P < 0.01, ***P < 0.001, as compared to vehicle control (One-way ANOVA with Dunnett's post-hoc test). VEH = vehicle, KET= ketamine, MDMA = (±)-3,4-methylenedioxymethamphetamine, PSI = psilocin.

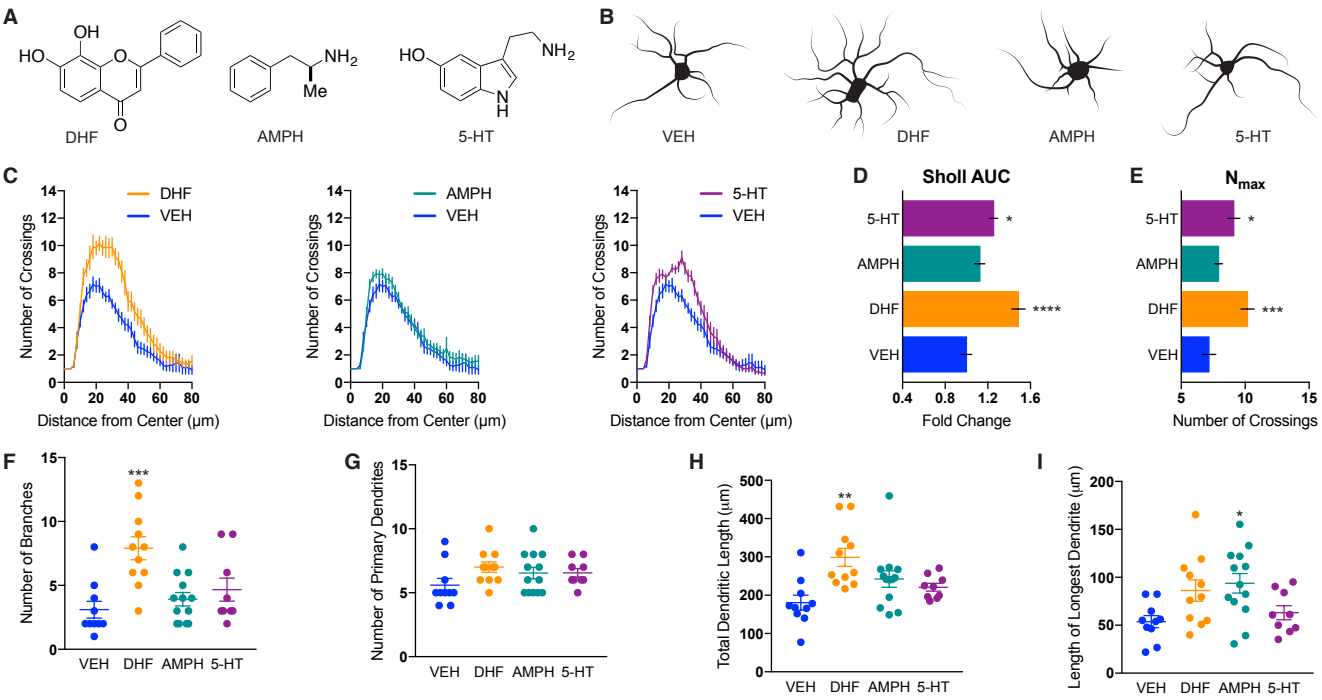


**Figure S2. Structural Plasticity is Promoted by a TrkB Agonist, but Not a Psychostimulant or Monoamine Neurotransmitter Structurally Related to Classical Psychedelics, Related to Figure 1.** (A) Chemical structures of control compounds used in these studies (DHF = positive control, AMPH and 5HT = negative controls). (B) Representative tracings of cultured embryonic rat cortical neurons (DIV6) treated with compounds. (C) Sholl analysis (circle radii = 2 μm increments) demonstrates that cultured cortical neurons treated with DHF, a TrkB agonist, have more complex dendritic arbors as compared to vehicle control. However, AMPH and 5-HT were not able to elicit a similar response (n = 9–13 neurons per treatment). (D) Area under the curve (AUC) of the Sholl plots in C. (E) Maximum number of crossings ($N_{max}$) of the Sholl plots in C. (F–I) Cultured cortical neurons treated with DHF, but not AMPH or 5-HT, exhibited an increased number of branch points (F) and total length of the dendritic arbor (H), but minimal changes in the number of primary dendrites (G) or the length of the longest dendrite (I). Error bars represent s.e.m. *P < 0.05, **P < 0.01, ***P < 0.001, ****P < 0.0001 as compared to vehicle control (One-way ANOVA with Dunnett's post-hoc test). VEH = vehicle, AMPH = D-Amphetamine, 5-HT = 5-hydroxytryptamine (serotonin), DHF = 7,8-dihydroxyflavone.

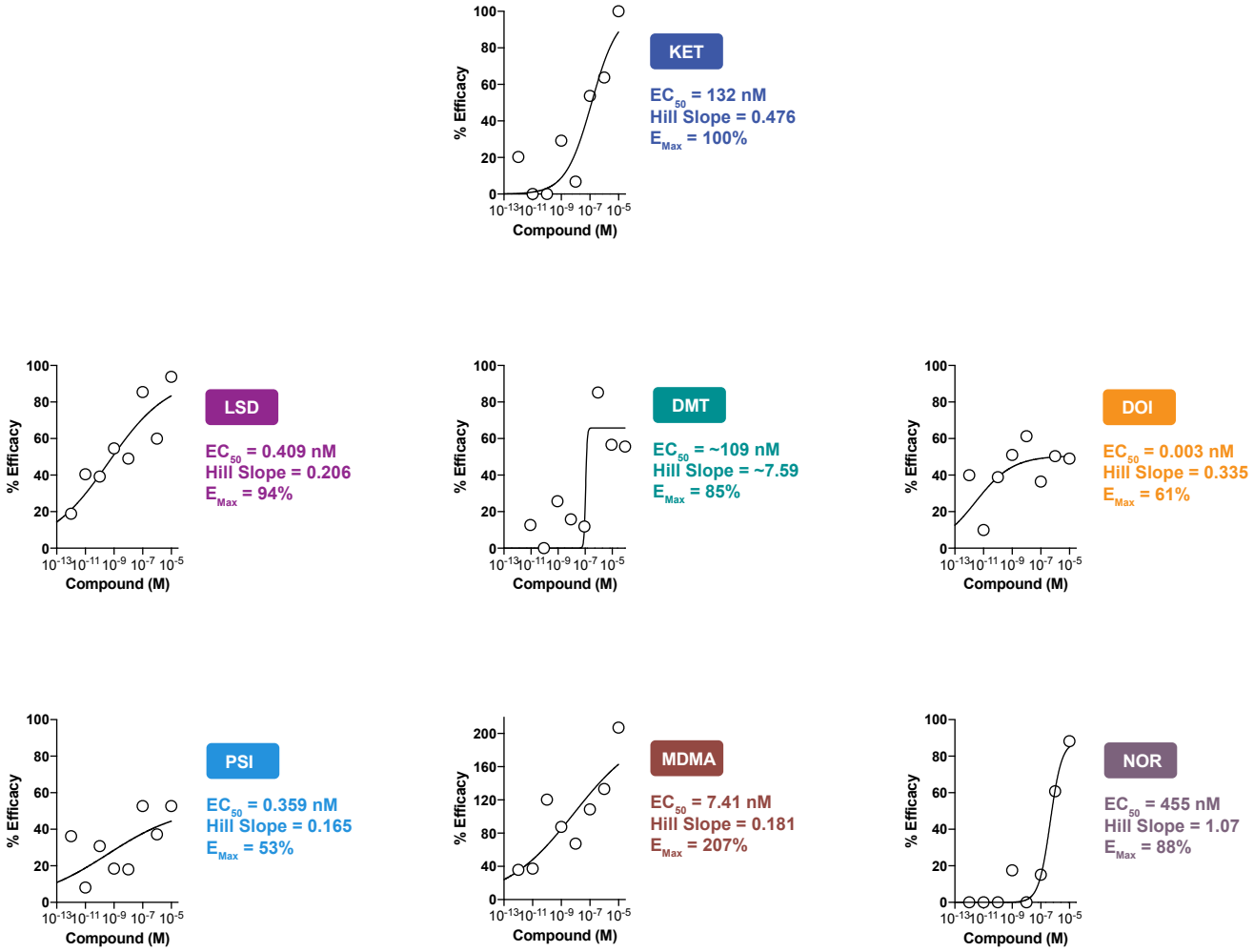


**Figure S3. Psychedelics Promote Neuritogenesis in a Dose-Dependent Manner, Related to Figure 1.** Cultured embryonic rat cortical neurons (DIV6) were treated with 8 decreasing concentrations of each compound (10-fold dilutions) and subjected to Sholl analysis. The $N_{max}$ values obtained following treatment with 10 μM ketamine and vehicle (0.1% DMSO) were defined as 100% and 0% respectively. The maximum number of crossings ($N_{max}$) of the Sholl plots are reported relative to these values. Using nonlinear regression analysis, $EC_{50}$ values and Hill slopes were calculated. Maximum efficacy relative to 10 μM ketamine is also shown. Most of the compounds display Hill slopes substantially different from 1, which suggests that this cellular phenotype is not mediated by binding to a single site and implies polypharmacology. KET = ketamine, LSD = lysergic acid diethylamide, DMT = N,N-dimethyltryptamine, DOI = (±)-2,5-dimethoxy-4-iodoamphetamine, PSI = psilocin, MDMA = (±)-3,4-methylenedioxymethamphetamine, NOR = noribogaine.

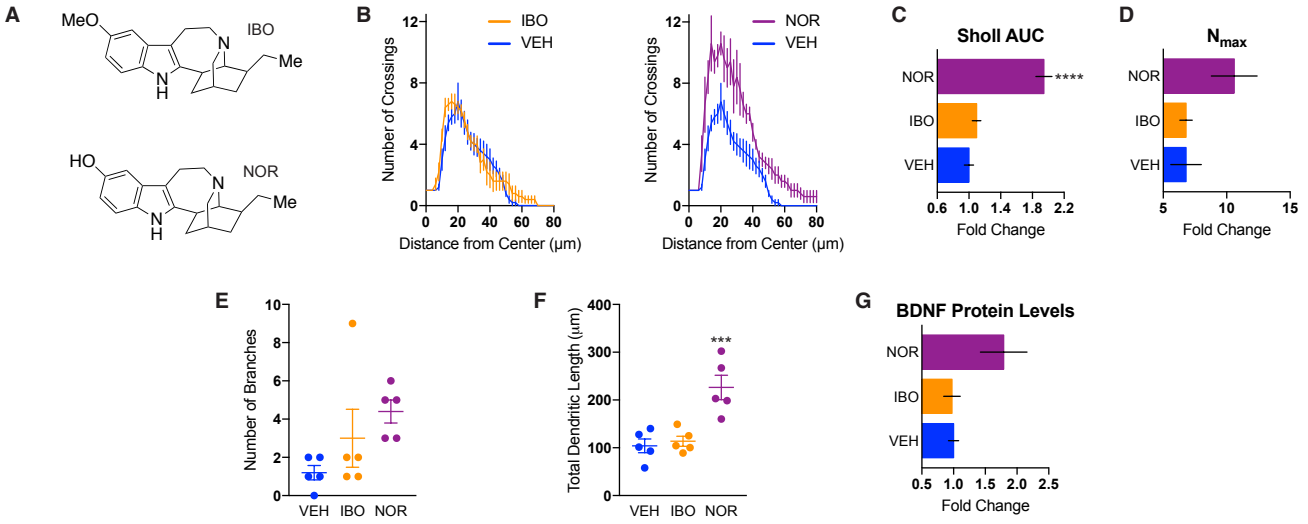


**Figure S4. Noribogaine, but Not ibogaine, Promotes Structural Neural Plasticity, Related to Figure 1.** (A) Chemical structures of the anti-addictive compound ibogaine and its metabolite noribogaine. (B) Sholl analysis (circle radii = 2 μm increments) demonstrates that cultured embryonic rat cortical neurons (DIV6) treated with noribogaine, but not ibogaine, have more complex dendritic arbors as compared to vehicle control (n = 5 neurons per treatment). (C) Area under the curve (AUC) of the Sholl plots in B. (D) Maximum number of crossings ($N_{max}$) of the Sholl plots in B. (E–F) Cultured cortical neurons treated with noribogaine, but not ibogaine, exhibited an increased number of branch points (E) and total length of the dendritic arbor (F). (G) Treatment with noribogaine, but not ibogaine, increases BDNF protein levels in DIV18 cultured cortical neurons after 24 h. Error bars represent s.e.m. *P < 0.05, **P < 0.01, ***P < 0.001, ****P < 0.0001 as compared to vehicle control (One-way ANOVA with Dunnett's post-hoc test). VEH = vehicle, IBO = Ibogaine, NOR = Noribogaine.

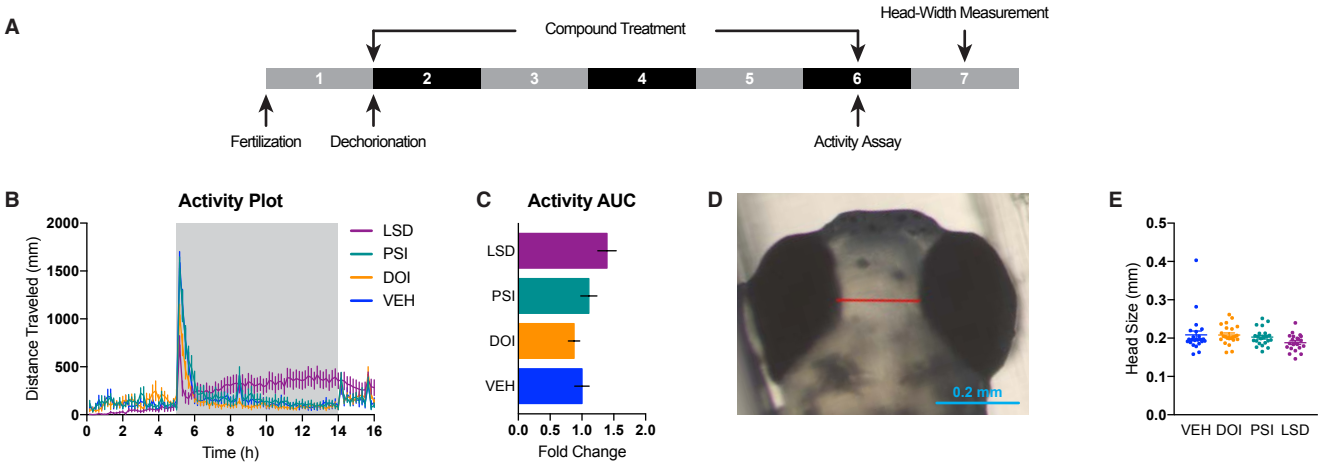


**Figure S5. Psychedelics Do Not Induce Behavioral or Gross Morphological Changes in Developing Zebrafish, Related to Figure 1.** (A) Experimental design used to assess the effects of psychedelics on zebrafish development. Alternating gray and black blocks represent individual days. Days are numbered in white. (B) Average activity of 5.5 dpf zebrafish (n = 23–24 zebrafish per treatment). The shaded area represents the dark period. A surge in activity immediately followed the transition from light to dark. (C) Area under the curve of the activity plot in B. (D) Representative example of a head-width measurement. (E) Treatment with psychedelics does not affect head size at 6.5 dpf. Error bars represent s.e.m. Treatments did not result in any significant differences as compared to vehicle control (One-way ANOVA with Dunnett's post-hoc test). VEH = vehicle, DOI = (±)-2,5-dimethoxy-4-iodoamphetamine, PSI = Psilocin, LSD = lysergic acid diethylamide, dpf = days post-fertilization.

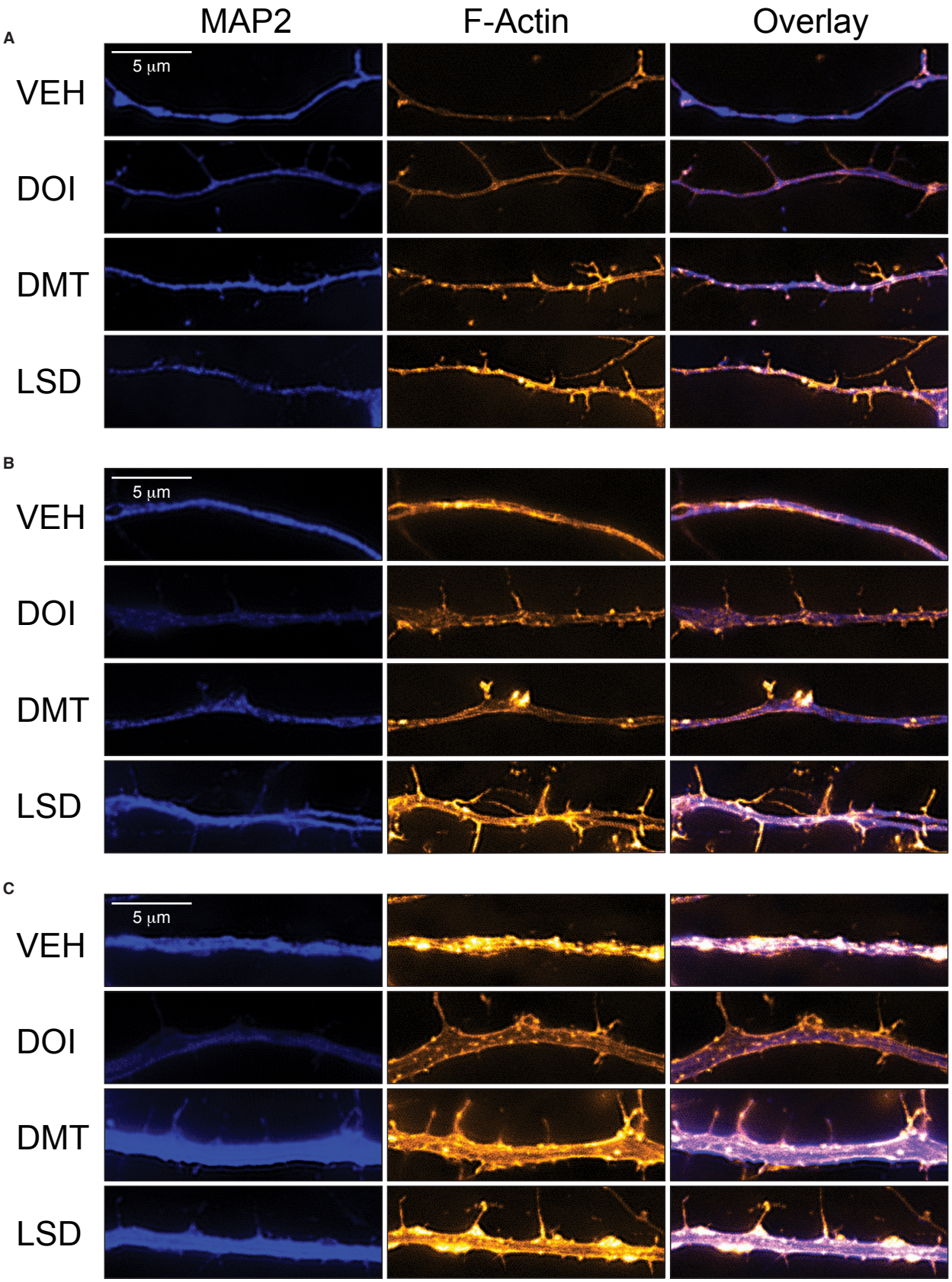


**Figure S6. Psychedelics Promote Spinogenesis in Cultured Cortical Neurons, Related to Figure 2.** (A–C) Representative super-resolution structured illumination microscopy (SIM) images of cultured embryonic rat cortical neurons (DIV19) treated with compounds for 24 h demonstrate that psychedelics promote spinogenesis (Blue = MAP2, Orange = F-actin). As MAP2 primarily labels the dendritic shaft while F-actin is found in all processes, orange protrusions from the shaft with minimal co-staining indicate dendritic spines. Examples of thin (A), medium (B), and thick (C) dendrites are presented.

## SUPPLEMENTAL METHODS

**Drugs.** The NIH Drug Supply Program provided (±)-2,5-dimethoxy-4-iodoamphetamine (DOI), lysergic acid diethylamide (LSD), ibogaine (IBO), noribogaine (NOR), (±)-3,4-metheylendioxymethamphetamine (MDMA), psilocin (PSI), and D-amphetamine (AMPH). Other chemicals were purchased from commercial sources such as ketamine hydrochloride (KET, Fagron), serotonin hydrochloride (5-HT, Alfa Aesar), 7,8-dihydroxyflavone (DHF, TCI), ANA-12 (MedChem Express), rapamycin (RAPA, Alfa Aesar), ketanserin (KETSN, ApexBio), and brain-derived neurotrophic factor (BDNF, Sigma-Aldrich). The fumarate salt of *N*,*N*-dimethyltryptamine (DMT), was synthesized in house as described previously (Cameron et al., 2018) and judged to be analytically pure based on NMR and LC-MS data.

**Neuritogenesis Experiments.** After 3 days in vitro (DIV3), approximately 50,000 cells/well in poly-D-lysine coated 24 well plates were treated. Treatment was accomplished by first diluting DMSO stock solutions of compounds 1:10 in Neurobasal followed by a 1:100 dilution into each well (total dilution = 1:1000). After 72 h, cells were fixed by removing 80% of the media and replacing it with a volume of 4% aqueous paraformaldehyde (Alfa Aesar) equal to 50% of the working volume of the well. Then, the cells were allowed to sit for 20 min at room temperature before the fixative was aspirated and each well washed twice with DPBS. Cells were permeabilized using 0.2% Triton X-100 (ThermoFisher) in DPBS for 20 minutes at room temperature without shaking. Plates were blocked with antibody diluting buffer (ADB) containing 2% bovine serum albumin (BSA) in DPBS for 1 h at room temperature. Then, plates were incubated overnight at 4ºC with gentle shaking in ADB and a chicken anti-MAP2 antibody (1:10,000; EnCor, CPCA-MAP2). The next day, plates were washed three times with DPBS and once with 2% ADB in DPBS. Plates were incubated for 1 h at room temperature in ADB containing an anti-chicken IgG secondary antibody conjugated to Alexa Fluor 488 (Life Technologies, 1:500) and washed five times with DPBS. After the final wash, 500 μL of DPBS was added per well and imaged on a Leica inverted epifluorescence microscope at 40x magnification. Images were analyzed using the Simple Neurite Tracer and Sholl analysis plug-ins for ImageJ Fiji (version 1.51N). Sholl analysis circle radii = 2 μm increments. All images were taken and analyzed by an experimenter blinded to treatment conditions.

For the dose response experiments (Figure S3) and two of the ketanserin blocking experiments (Figure 6G and H), a slightly modified method was employed. Neurons were cultured at approximately 15,000 cells/well in poly-D-lysine coated 96-well plates. For the dose response studies, neurons were treated at DIV3 by removing 10% of the media and replacing that with a 10x solution of compound in Neurobasal to reach the desired concentrations (final concentration of DMSO = 0.1%). For the ketanserin blocking experiments, the media was replaced on DIV3 with “replacement media” containing ketanserin. After 10 mins, compounds dissolved in Neurobasal were added to yield final concentrations of experimental compound and ketanserin (final concentration of DMSO = 0.2%). On DIV6, cells were fixed and imaged as described above. Plates were imaged on a Molecular Devices ImageXpress Micro XLS Widefield High-Content Analysis System at 9 sites per well using 20x magnification. Images were analyzed using ImageJ Fiji (version 1.51N). All analysis was done by an experimenter blinded to treatment conditions.

**Spinogenesis Experiments.** Cells were plated at a density of 35,000 cells/well on glass coverslips in 24 well plates. At DIV18, cells were treated for 24 h and fixed as described for the neuritogenesis experiments (vide supra). Fixative was aspirated and each well washed twice with DPBS. Cells were permeabilized using 0.2% Triton X-100 (ThermoFisher) in DPBS for 20 minutes at room temperature without shaking. Plates were blocked with antibody diluting buffer (ADB) containing 2% bovine serum albumin (BSA) in DPBS for 1 h at room temperature. Then, plates were incubated overnight at 4ºC with gentle shaking in ADB and anti-chicken MAP2 (1:10,000; EnCor, CPCA-MAP2). The next day, plates were washed three times with DPBS and once with 2% ADB in DPBS. Plates were incubated for 1 h at room temperature in ADB containing an anti-chicken IgG secondary antibody conjugated to Alexa Fluor 568 (Life Technologies, 1:500) and phalloidin conjugated to Alexa Fluor 488 (Life Technologies, 1:40). Then, the cells were washed five times with DPBS. Finally, the coverslips were mounted onto microscope slides using ProLong Gold (Life Technologies) and allowed to cure for 24 hours at room temperature. Images of secondary dendrites were taken using a Nikon N-SIM Structured Illumination Super-resolution Microscope with a 100x/NA 1.49 objective, 100 EX V-R diffraction grating, and an Andor iXon3 DU-897E EMCCD. Images were recollected and reconstructed in the “2D-SIM” mode (no out of

focus light removal; reconstruction used three diffraction grating angles each with three translations). Dendritic spines were counted manually by a trained experimenter who was blinded to the treatment conditions.

**Synaptogenesis Experiments.** Cells were plated at a density of 35,000 cells/well on glass coverslips in 24 well plates. At DIV18, cells were treated for 24 h and fixed as described for the neuritogenesis experiments (vide supra). Fixative was aspirated and each well washed twice with DPBS. Cells were permeabilized using 0.2% Triton X-100 (ThermoFisher) in DPBS for 20 minutes at room temperature without shaking. Plates were blocked with antibody diluting buffer (ADB) containing 2% bovine serum albumin (BSA) in DPBS for 1 h at room temperature. Then, plates were incubated overnight at 4ºC with gentle shaking in ADB and anti-MAP2 (1:10,000; EnCor, CPCA-MAP2), anti-VGLUT1 (Millipore, AB5905, 1:1000), and anti-PSD-95 (Millipore, MABN68, 1:500) antibodies. The next day, plates were washed three times with DPBS and once with 2% ADB in DPBS. Plates were incubated for 1 h at room temperature in ADB containing secondary antibodies conjugated to Alexa Fluor 488 (Life Technologies, 1:500), Cy3 (Jackson ImmunoResearch Inc, 1:500), or Alexa Fluor 647 (Jackson ImmunoResearch Inc, 1:500). Images of secondary dendrites were collected using a confocal microscope (Olympus FV1000) with a 60x oil objective and a 1.42 numerical aperture.

Synaptic density and size as well as PSD-95 and VGLUT1 densities were determined using custom software that works in three stages. The first stage is a foreground/background separation that outputs a mask of pixels within the image that correspond to the neuron. Next, puncta of synaptic proteins are identified using only pixels belonging to the foreground mask from the first stage. Finally, synapses are identified as colocalizations of puncta of pre- and post-synaptic proteins. The foreground mask is determined using a fluorescence intensity threshold chosen to maximize the connectedness of both the foreground and the background. Specifically, for a given threshold, connected pixels that pass the threshold are clustered together, and connected pixels that fall below threshold are clustered together. The average cluster size is computed for each type of cluster, and the threshold that maximizes the product of these averages is chosen. The resulting foreground mask is cleaned by removing clusters smaller than 0.06 $\mu m^2$ and smoothed by eliminating pixels connected to fewer than three other pixels that passed the threshold and adding pixels connected to more than four pixels that passed the threshold. Within the foreground mask, every pixel that has greater intensity than its neighbors is treated as a seed point for a potential punctum. The median and standard deviation of pixel intensities is computed for foreground pixels in the neighborhood of each seed point. The size of the local neighborhood is made dynamic in order to maintain sufficient statistics, with a minimum size of 5 $\mu m^2$. Seed points with intensities less than 3 standard deviations above the local median are rejected. For seed points that pass this threshold, adjacent pixels that pass a less stringent threshold (the minimum of 2 standard deviations above the median and the average of the median and seed point intensities) are clustered. In order to prevent neighboring puncta from being clustered together, intensities for newly added pixels are required to decrease if adjacent established pixels are already close to the lower threshold. Once the clustering is complete, puncta are smoothed in the same manner as the foreground and rejected if they are smaller than 0.03 $\mu m^2$. Pixels that are part of a punctum passing all of the above criteria are removed from the foreground mask so as not to be included in the threshold calculation for future puncta. After every seed point has been tested, those that failed are iterated over again until no new puncta are added. At the beginning of each iteration, puncta smaller the 3 times the minimum size threshold are removed to be reclustered. Synapses are defined as a colocalization of PSD-95 and VGLUT1 puncta. Two puncta are considered colocalized if they have at least 1 pixel of overlap. Synapse densities as well as the densities of presynaptic and postsynaptic markers are calculated using dendrite areas computed by counting pixels within a region of interest belonging to the foreground mask in the MAP2 channel. A similar approach for calculating synapse density has been described previously (Nielend et al., 2014). Synapse size was calculated using the number of pixels representing each colocalization event. Outliers were removed using the ROUT method in GraphPad Prism (version 7.0a) with a Q value equal to 5%.

**ELISA.** Cortical cultures were grown in 6-well plates (600,000 cells per well). At DIV17-18, all media was removed and replaced with fresh Neurobasal. After 4 h, each well was treated with compound dissolved in DMSO (1:1000) for 24 h. After the treatment period, the media was removed and the cells washed once with ice-cold DPBS. To each well was added 200 µL of Cell Extraction Buffer (Life Technologies) supplemented with cOmplete and PhoSTOP inhibitors, and incubated on ice for 5–10 min. Plates were scrapped and the contents collected. The samples were centrifuged at 10,000 x g for 10 min at 4 ºC and subjected to a BDNF

ELISA assay (ThermoFisher) as per the manufacturer's protocol with the exception that the colorimetric signal was only allowed to develop for 8 minutes.

**ddPCR.** Cortical cultures were grown in 6-well plates (600,000 cells per well) until DIV17-18. At that time, cells were treated with compounds (1:1000 dilution from DMSO stock solutions) for 24h. Cells were then lysed using QIAzol Lysis Reagent (QIAGEN) and RNA extracted using the RNeasy isolation kit (QIAGEN) following instructions of the manufacturer. The resulting RNA was converted to cDNA using the iScript cDNA Synthesis Kit (BioRad). Droplets containing PCR master mix and taqman probes for BDNF (ThermoFisher, RN02531967_s1) and ESD (ThermoFisher, RN01468295_g1) were generated using the QX200 Droplet Digital PCR System (BioRad). Following PCR amplification, BDNF signal was quantified and normalized to the housekeeping gene ESD.

**5-HT2A Staining Experiments.** Cells were plated at a density of 35,000 cells/well on glass coverslips in 24 well plates. At DIV6 and DIV19, cells were fixed as described for the neuritogenesis experiments (vide supra). Fixative was aspirated and each well washed three times with DPBS. Cells were permeabilized and blocked using 0.1% Triton X-100 (ThermoFisher) and 5% goat serum (Vector Labs S-1000) in DPBS (TPG) for 1 hour at room temperature with gentle shaking. Plates were incubated overnight at 4 ºC with gentle shaking with anti-MAP2 (1:1000) and rabbit anti-5-HT2A (Millipore Sigma PC176, 1:100) antibodies diluted in TPG. The next day, plates were washed three times for 5 min each with wash buffer (0.1% Triton X-100 in DPBS). Plates were incubated for 1 hour at room temperature in TPG containing secondary antibodies conjugated to Oregon Green 488 (Life Technologies, 1:500) and Alexa Fluor 568 (Life Technologies, 1:500). Plates were again washed three times for 5 min each with wash buffer (0.1% Triton X-100 in DPBS) and post-fixed for 10 min with 4% PFA in DPBS. Cells were washed three times with DPBS and mounted onto microscope slides using Prolong Gold (Life Technologies). After curing for 24 hours at room temperature, images of neurons were collected using a confocal microscope (Olympus FV1000) with a 60x oil objective (1.42 NA).

The anti-5-HT2A antibody used in these studies (i.e., Millipore Sigma PC176) was produced using a peptide antigen corresponding to residues 22–41 of the rat 5-HT2A receptor. The specificity of an antibody produced using the same antigen has been validated previously (Garlow et al., 1993). As it was unclear from the manufacturer's information whether or not the antibody utilized in our studies was produced using the same carrier protein (McDonald and Mascagni, 2007), we performed our own validation experiments. Briefly, HEK293T cells (ATCC, CRL-3216) and 198A2 cells (i.e., a HEK293 cell line stably expressing 5-HT2A receptors, donated by Javier González-Maeso; see González-Maeso et al., 2003; Ebersole et al., 2003) were fixed, stained, and imaged with a 100x oil objective (1.3 NA) on an inverted widefield microscope (Leica DMIL). Representative bright-field images (grayscale) overlaid with fluorescence images (green) indicating 5-HT2A expression are shown below. The cells expressing 5-HT2A receptors exhibit significantly more fluorescence and the expected staining at the cell membrane (white arrow), validating this antibody for immunofluorescence studies.

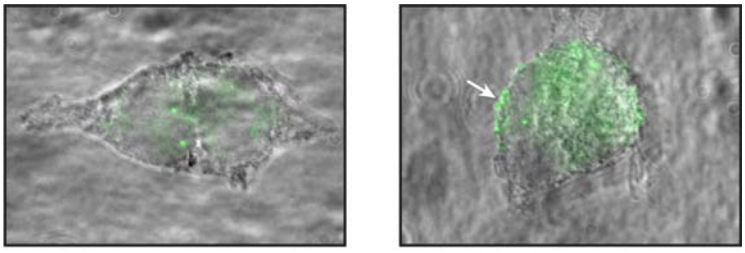

HEK293T
(Does Not Express 5-HT2A)

1988A
(Stably Expresses 5-HT2A)

**Drosophila Experiments.** For morphological analysis, we crossed *221-Gal4* with *UAS-cd4-tdGFP*, collected the progeny at either the first larval instar (early treatment) or late second larval instar (late treatment), then transferred the larvae to grape agar plates smeared with yeast paste. This yeast paste was dissolved in 1 mL of autoclaved water containing 0.1% DMSO with or without compounds dissolved at concentration of 10 μM. Whole, live wandering third instar larvae were mounted in 90% glycerol under coverslips sealed with grease and imaged using an Olympus FV1000 laser scanning confocal microscope. For fly stocks, we used the Gal4 driver line, *221-Gal4* (Grueber et al., 2003), to drive the expression of the membrane marker, *UAS-cd4-tdGFP*

(Han et al., 2011), to visualize dendrite morphology for all conditions. Collected Z-stacks containing the dendritic arbors of the class I da sensory neurons were used for analysis. One neuron from segment A3 or A4 was imaged per larvae and three larvae were imaged per drug condition per treatment window (early vs. late treatment). All larval drug treatments were performed at least three separate times. Total dendrite length and the number of branch points were determined from maximum Z projections of the Z-stack image files using the Simple Neurite Tracer plugin for ImageJ Fiji (Longair et al., 2011). Data acquisition and analysis was performed by an experimenter blinded to treatment conditions.

**Zebrafish Experiments.** Wildtype fish (NHGRI-1) were dechorionated 24 h post fertilization (hpf) and placed individually into a 96-well plate containing chemicals of interest (10 μM compound, 0.1% DMSO). Larvae were raised in a light-cycled incubator (28°C) and subsequently subjected to an activity assay for 16 hours, from 5pm to 9am, at 5.5–6.5 days post fertilization (dpf). Specifically, they were imaged using DanioVision with a light cycle mimicking their natural day/night cycle. Subsequently, fish larvae (6.5 dpf) were immediately fixed following the movement assay using 4% aqueous paraformaldehyde overnight. Head-width measurements were performed by imaging larvae dorsally using a stereomicroscope (12x magnification) and a digital ruler (ImageJ) to measure the distance between the inner edges of each eye. Data acquisition and analysis was performed by an experimenter blinded to treatment conditions.

**Golgi-Cox Staining.** Female Sprague Dawley rats (~8 weeks old) were given an intraperitoneal injection of DMT, ketamine, or vehicle and sacrificed via decapitation 24 h later. Tissue was prepared following the protocol outlined in the FD Neurotechnologies Rapid GolgiStain Kit (FD Neurotechnologies) with slight modifications. Brains were stored in solution C for 2 months prior to slicing into 120 μm sections using a vibratome. These slices were placed onto microscope slides that were pre-coated with (3-aminopropyl)triethoxysilane. Slices were air dried for a week before staining. Slides were immersed in water twice for 2 minutes, DE solution for 10 minutes, and then water for 2 minutes. After this, slides were immersed sequentially in 25% ethanol for 1 minute, 50% ethanol for 4 minutes, 75% ethanol for 4 minutes, 95% ethanol for 4 minutes, and 100% ethanol for 4 minutes. Slides were then briefly dipped into xylenes before being mounted using DPX Mountant For Histology (Sigma), air-dried, and imaged on a Zeiss AxioScope. Spines were traced in three dimensions using Neurolucida software (version 10) at 100x magnification. Data acquisition and analysis was performed by an experimenter blinded to treatment conditions. Data represents individual neurons taken from 3 different animals per treatment.

**Electrophysiology.** Female Sprague Dawley rats (~8 weeks old) were given an intraperitoneal injection of DMT or vehicle. After 24 h, rats were anesthetized with isofluorane and transcardially perfused with ice-cold artificial cerebrospinal fluid (ACSF), containing 119 mM NaCl, 26.2 mM $NaHCO_3$, 11 mM glucose, 2.5 mM KCl, 1 mM $NaH_2PO_4$, 2.5 mM $CaCl_2$ and 1.3 mM $MgSO_4$. Brains were rapidly removed and 300 μm coronal slices from the mPFC were cut on a Leica VT1200 vibratome (Buffalo Grove, IL) with ice-cold ACSF solution. Slices were incubated in 32 °C NMDG solution for 10 minutes, transferred to room temperature ACSF, and held for at least 50 minutes before recording. All solutions were vigorously perfused with 95% $O_2$ and 5% $CO_2$. Spontaneous excitatory postsynaptic currents (sEPSCs) were recorded at -70 mV in 32 °C ACSF. Cells were patched with 3–5 MΩ borosilicate pipettes filled with intracellular solution containing 135 mM cesium methanesulfonate, 8 mM NaCl, 10 mM HEPES, 0.3 mM Na-GTP, 4 mM Mg-ATP, 0.3 mM EGTA, and 5 mM QX-314 (Sigma, St Louis, MO). Series resistance was monitored throughout experiments; cells were discarded if series resistance varied more than 25%. All recordings were obtained with a Multiclamp 700B amplifier (Molecular Devices, Sunnyvale, CA). Analysis was performed with the Mini Analysis program (Synaptosoft, Decatur, GA) with a 4 pA detection threshold. Data represents individual neurons taken from 3 different animals per treatment. Data acquisition and analysis was performed by experimenters blinded to treatment conditions.

**Code Availability.** The code used to generate synaptogenesis data is available from the corresponding author upon reasonable request.

**Data Availability.** The data that support the findings of this study are available from the corresponding author upon reasonable request.

**Supplemental References.**


Ebersole, B.J., Visiers, I., Weinstein, H., and Sealfon, S. C. (2003). Molecular basis of partial agonism: orientation of indoleamine ligands in the binding pocket of the human serotonin 5-HT2A receptor determines relative efficacy. Mol. Pharmacol. *63*, 36–43.

Garlow, S.J., Morilak, D.A., Dean, R.R., Roth, B.L., and Ciaranello, R.D. (1993). Production and characterization of a specific 5-HT2 receptor antibody. Brain Res. *615*, 113–120.

Grueber, W.B., Ye, B., Moore, A.W., Jan, L.Y., and Jan, Y.N. (2003). Dendrites of distinct classes of Drosophila sensory neurons show different capacities for homotypic repulsion. Curr. Biol. *13*, 618–626.

Han, C., Jan, L.Y., and Jan, Y.N. (2011). Enhancer-driven membrane markers for analysis of nonautonomous mechanisms reveal neuron-glia interactions in Drosophila. Proc. Natl. Acad. Sci. USA *108*, 9673–9768.

Longair, M.H., Baker, D.A., and Armstrong, J.D. (2011). Simple Neurite Tracer: open source software for reconstruction, visualization and analysis of neuronal processes. Bioinformatics *27*, 2453–2454.

McDonald, A.J., and Mascagni, F. (2007). Neuronal localization of 5-HT type 2A receptor immunoreactivity in the rat basolateral amygdala. Neuroscience *146*, 306–320.

Nieland, T.J., Logan, D.J., Saulnier, J., Lam, D., Johnson, C., Root, D.E., Carpenter, A.E., and Sabatini, B.L. (2014). High content image analysis identifies novel regulators of synaptogenesis in a high-throughput RNAi screen of primary neurons. PLoS One *9*, e91744

González-Maeso, J., Yuen, T., Ebersole, B.J., Wurmbach, E., Lira, A., Zhou, M., Weisstaub, N., Hen, R., Gingrich, J.A., and Sealfon, S.C. (2003). Transcriptome fingerprints distinguish hallucinogenic and nonhallucinogenic 5-hydroxytryptamine 2A receptor agonist effects in mouse somatosensory cortex. J. Neurosci. *23*, 8836–8843.